JOURNAL OF SOLID STATE CHEMISTRY **133,** 458–465 (1997)
ARTICLE NO. SC977510

^{121}Sb Mössbauer Study of Sb_2S_3–As_2S_3–Tl_2S Glasses

J.-M. Durand,*,‡ M. A. El Idrissi-Raghni,* J. Olivier-Fourcade,* J.-C. Jumas,*,[1] and G. Langouche†

*Laboratoire de Physicochimie de la Matière Condensée (UMR 5617 CNRS), Université Montpellier II—Sciences et Techniques du Languedoc, Place Eugène Bataillon, 34095 Montpellier Cedex 5, France; †Instituut voor Kern- en Stralingsfysika, Katholieke Universiteit Leuven, 200D Celestijnenlaan, 3030 Leuven, Belgium; and ‡Institut de Ciència de Materials de Barcelona, Campus de la Universitat Autònoma de Barcelona, 08193 Bellaterra, Spain

Received November 13, 1996; in revised form June 11, 1997; accepted June 12, 1997

The local environment of antimony atoms in vitreous samples of the ternary system Sb_2S_3–As_2S_3–Tl_2S is studied by ^{121}Sb Mössbauer spectroscopy. The results have been interpreted by means of EBV (empirical bond valence) and EBLV (empirical bond length valence) calculations. Variations in isomer shifts are attributed to changes in the environment of antimony atoms. The isomer shift is found to be a very sensitive parameter reflecting variations in the mean coordination number and in the mean Sb–S bond length. The results presented here confirm the random substitution of As by Sb in the binary system As_2S_3–Sb_2S_3 and the competitive effects—breaking of As–S–As bridges by Tl and formation of As–S–Sb bridges—in the ternary system Sb_2S_3–As_2S_3–Tl_2S, in agreement with previous XAFS studies.

1. INTRODUCTION

There is currently increasing interest in chalcogenide glasses due to their optical properties (transparency in the IR, optical fibers) and their applications in data processing (electronic switches, optical memories) (1–5) as well as in solar cells (6). Especially the possibility to prepare low-cost heterojunctions on the basis of *p*-Si has directed wide interest toward Sb_2S_3 (6). The need of a deeper understanding of the relationship between structure on one side and electrical and optical properties on the other side explains the currently increasing number of studies on Sb_2S_3 and its solid solutions with other chalcogenides (4). Structural studies are of particular importance in this context, since electrical and optical properties are strongly influenced by short-range order around the metal atom. The number of experimental methods giving reliable information on short-range order in glasses is, however, limited. Mössbauer spectroscopy is one of the experimental methods that can be usefully applied for this purpose.

In previous papers (7–11), we have reported on a study of the ternary system As_2S_3–Sb_2S_3–Tl_2S, which is of particular interest due to its wide domain of glass formation. These previous studies by means of XAFS (X-ray absorption fine structure) (8–10) and by far-infrared transmission spectroscopy (11) have revealed the possibility of varying considerably the structural features of the glasses belonging to this system by changing their stoichiometry. The structural variety is due to the strongly different properties of the three basic binary sulfides. As_2S_3 and Sb_2S_3 are both glass-forming compounds, while Tl_2S is a glass modifying compound. Arsenic usually obeys the "8-*N*" rule, which means that its coordination number is determined by the number of electrons needed to complete its valence shell. Arsenic is therefore found in a pyramidal AsS_3E-type environment (8), *E* being the 4*s* nonbonding electrons. These electrons are, despite their chemical inactivity, influenced by the ligands. In distorted octahedra with some of the ligands considerably farther away from the central atom or even completely missing, the *ns* distribution ($n = 4$ for As and $n = 5$ for Sb) is admixed with other states and looses its sphericity. The *ns* density tends to fill out a part of the space that is left vacant by the missing ligands as shown in Fig. 1. This behavior is referred to as stereochemical activity of the nonbonding electrons *E* (12). Antimony does not obey the "8-*N*" rule and can be found, at least in the compounds studied here, in three coordination patterns which are shown in Fig. 1: the pyramidal SbS_3E type, the triangle-based bipyramidal SbS_4E type, and the square-based pyramidal SbS_5E types. The stereochemical activity of the nonbonding electrons decreases with increasing coordination number (12).

The XAFS studies at different absorption edges already gave insight into the structural modifications that can be achieved by each of the three basic compounds. It has been shown that the binary system As_2S_3–Sb_2S_3 is characterized by a random substitution of arsenic by antimony, in agreement with a model proposed earlier by Bychkov and Wortmann (13). Thallium sulfide has been found to crack the As–S–As bridges present in the As_2S_3 host matrix and to

[1] To whom correspondence should be addressed.

0022-4596/97 $25.00

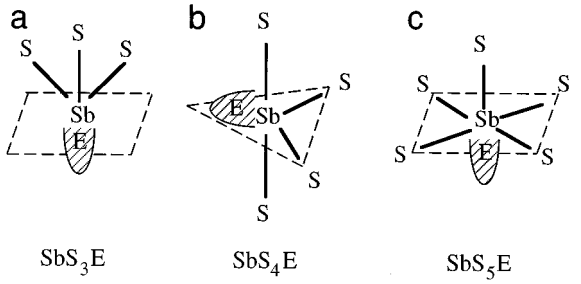

FIG. 1. Possible coordination patterns of antimony: (a) pyramidal SbS_3E coordination, (b) triangular-based bipyramidal SbS_4E coordination, (c) square-based pyramidal SbS_5E coordination.

lead to terminal As–S bonds, which confirms the results of Heo *et al.* (14). In the small domain of glass formation of the Sb_2S_3–Tl_2S binary system, the vitreous compounds are principally composed of the pyramidal SbS_3E units. This picture is altered when all three sulfides are present simultaneously. Adding Sb_2S_3 to an already Tl_2S-doped As_2S_3 matrix reduces the number of terminal As–S bonds by virtue of the formation of As–S–Sb bridges with SbS_4E and SbS_5E units. Introduction of As_2S_3 into a Sb_2S_3 matrix already containing Tl_2S leads to a higher fraction of SbS_4E and SbS_5E units.

The aim of this paper is to complete the investigation of the As_2S_3–Sb_2S_3–Tl_2S system by a study of ^{121}Sb Mössbauer, which gives information through the isomer shift on the *s*-electron density remaining at the Sb nucleus and through the quadrupole coupling, which reflects the electric field gradient, on the electronic distribution.

2. EXPERIMENTAL

Synthesis and characterization of the vitreous samples in the ternary system As_2S_3–Sb_2S_3–Tl_2S were previously described (8–10).

The ^{121}Sb Mössbauer measurements were carried out in standard transmission geometry using a ^{121m}Sn in $BaSnO_3$ source. During the measurements, both source and absorbers were simultaneously cooled down to liquid helium temperature to increase the fraction of recoil-free absorption and emission processes. The velocity scale was calibrated with the standard spectrum of an iron absorber obtained using a ^{57}Co source. The zero isomer shift was defined from the spectrum of the reference InSb. It should be mentioned that the calibration and the zero isomer shift were checked carefully, since the relative changes of the isomer shift and the electric quadrupole coupling constant from one sample to another were relatively small.

3. BACKGROUND

Antimony atoms have an electronic configuration $[Kr]4d^{10}5s^25p^3$ and are found in oxidation states III and V. In its compounds with elements of column VI (S, Se, and Te), antimony atoms are in most cases found in the oxidation state III. These antimony(III) chalcogenides are characterized by a $5s^2$ nonbonding electrons. The Sb(III) atoms characteristically show very irregular coordination in their crystalline complexes (12).

In this discussion, we introduce the term valence which is taken to be the formal oxidation state or ionic charge of an atom. Where an atom forms many bonds, this potential must be shared between them. Following Pauling (15), we can define the average bond strength, or average bond valence, as being equal to the atom valence divided by the coordination number. Where the bonds are all equivalent the individual bond valences will be equal to the average. In the other cases, the valence may be unequally shared between the various bonds and in such cases the individual bond valence is the amount of an atom's potential for bonding that is associated with a particular bond.

A number of authors (16–18) have shown that the length of a bond is inversely related to its bond valence, and Brown and Shannon (18) have used the principle that the sum of the bond valences around each atom must be equal to the atom valence. They define and calculate an empirical bond valence S from the observed bond lengths R with the relation

$$S = S_0(R/R_0)^{-N}, \qquad [1]$$

where S_0, R_0, and N are constants for a given pair of atoms. Brown (19) has determined the relation for different couples of A and B atoms where A = Sn(II), Sb(III), Te(IV), and I(V) and B = O and F by using the bond lengths observed in various crystals. In this study, we determined the values of the three constants for the pair (Sb, S). To this end, we investigated different environments of the antimony atoms in various crystalline compounds of the binary system Sb_2S_3–Tl_2S. In this system, five crystalline compounds can be found: Sb_2S_3, $TlSb_5S_8$, $TlSb_3S_5$, $TlSbS_2$, and Tl_3SbS_3. In all five cases, the crystalline structures, atomic positions, and bond lengths are well known from X-ray diffraction. In the following description of antimony environments, we took into account the bonds smaller than 2.90 Å. We must also point out several weak bonds (with bond lengths between 2.90 and 3.60 Å) of various antimony environments.

In Sb_2S_3 (20), antimony is found on two different crystallographic sites. One is of the pyramidal-type SbS_3E with bond lengths between 2.52 and 2.54 Å, and the other is of the square-based pyramid-type SbS_5E with bond lengths between 2.46 and 2.85 Å. In $TlSb_5S_8$ (21, 22), antimony occupies ten crystallographically different sites: six with an SbS_3E environment (bond lengths between 2.41 and 2.58 Å), three of the triangle-based bipyramidal-type SbS_4E (2.40–2.90 Å), and one of the SbS_5E type (2.44–2.75 Å). The compound $TlSb_3S_5$ (22, 23) has three different antimony sites: two of them are of the SbS_3E type (2.43–2.61 Å), and the

third is of the SbS_4E type (2.44–2.85 Å). In $TlSbS_2$ (24), we have to deal with two different antimony sites, one of the SbS_3E type (2.41–2.61 Å) and one of the SbS_4E type (2.43–2.81 Å). Finally, in Tl_3SbS_3 (25), antimony is found on one crystallographic site of the pyramidal SbS_3E type with equal bond lengths (2.43 Å).

To determine the constants S_0 and R_0, the compound with the simplest structure is chosen: Tl_3SbS_3 with only one antimony site and three sulfur atoms at the same bond length (2.43 Å). The sum of the bond valence around each atom must be equal to the atom valence ($V_{Sb} = 3$), and the values of S_0 ($S_0 = 3/3 = 1$) and of R_0 ($R_0 = 2.43$ Å) can be deduced. For the determination of the constant N, we calculated its value using the two antimony environments in the compound $TlSbS_2$ because for both environments there are only four bonds with lengths smaller than 3.0 Å and no bond of length between 3.0 and 3.6 Å. Hence we cannot hesitate for the calculation on the choice of limits of the bond lengths. Best agreement with the atom valence is obtained for $N = 5.2$. Thus the relation for the empirical bond valence proposed for the pair (Sb, S) is the following:

$$S = (R/2.43)^{-5.2}. \qquad [2]$$

We verified the relation on other crystalline compounds and in particular on the three other crystalline compounds of the Sb_2S_3–Tl_2S binary system, Sb_2S_3, $TlSb_5S_8$, and $TlSb_3S_5$. In this calculation, we took Sb–S bond lengths smaller than 3.2 Å into account. If we take into account bonds with lengths higher than 3.20 Å, the sums of the empirical bond valences for many antimony environments become distinctly larger than 3. For the compounds Sb_2S_3, $TlSb_5S_8$, and $TlSb_3S_5$, we calculated the values of 3.00, 3.08, and 3.12, respectively. Brown (19) had found that the sums of the empirical bond valences came within 4% of the atomic valence in the large number of crystal structures they had examined. Below we shall distinguish the Sb–S strong bonds with lengths smaller than 2.90 Å (these bonds allow the description of antimony environments) and the weak bonds with lengths between 2.90 and 3.20 Å.

4. RESULTS AND DISCUSSION

The left panel of Fig. 2 shows the positions of the crystalline compounds studied here within the Sb_2S_3–As_2S_3–Tl_2S phase diagram, where the shaded area represents the domain of glass formation. The right panel shows the positions of the amorphous compounds with their numbering used throughout this paper. We investigated by ^{121}Sb Mössbauer spectroscopy the five crystalline compounds of the Sb_2S_3–Tl_2S binary system and several glasses of the Sb_2S_3–As_2S_3 binary system. In the Sb_2S_3–As_2S_3–Tl_2S ternary system two series of samples with the constant Tl_2S concentrations of 20% and 40% were included in the study. The Mössbauer transition for the ^{121}Sb isotope is of type $\frac{5}{2} \rightarrow \frac{7}{2}$. Broad asymmetric lines indicating unresolved quadrupole split spectra are observed for all samples. As the relative variation of the nuclear radius, $\Delta R/R$, is rather large (26, 27), in the case of ^{121}Sb, although the nuclear quadrupole moment Q is rather small, the ^{121}Sb isomer shift is a more sensitive parameter to changes of the local environment than is the electric quadrupole coupling constant. As a consequence, a distribution of the electric quadrupole coupling constants, as it would be expected from the various different environments in antimony glasses, is not reliably resolved. All spectra were therefore fitting supposing only one antimony site, although in almost all crystalline (except for the crystalline compound Tl_3SbS_3) and vitreous compounds, several different environments are present. Thus, all values of isomer shifts and electric quadrupole coupling constants presented here should be regarded as averaged. The hyperfine interaction parameters (isomer shift δ, electric quadrupole coupling constant eQV_{zz}, and linewidth W) are summarized in Tables 1 and 2. The isomer shifts are

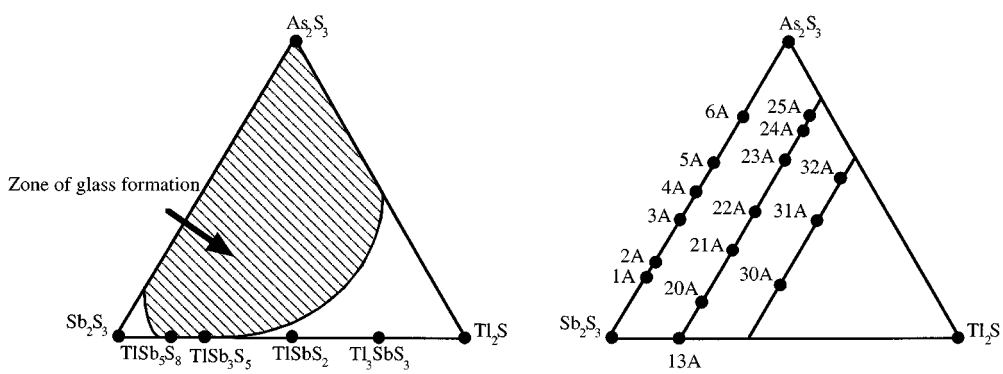

FIG. 2. (Left Panel) Crystalline compounds in the Sb_2S_3–As_2S_3–Tl_2S ternary system and zone of glass formation. (Right Panel) Positions within this system of the amorphous samples studied here, given with their numbering used throughout this paper.

TABLE 1

Summary of Isomer Shifts, δ (with Respect to InSb), Electric Quadrupole Coupling Constants, eQV_{zz}, Linewidth, Γ, Resulting from a Least-Squares Analysis of the Mössbauer Data, Mean Bond Length, and Mean Coordination Number for the Crystalline Compounds of the Sb_2S_3–Tl_2S Binary System

Crystalline compounds	% Sb_2S_3	δ (mm/s)	eQV_{zz} (mm/s)	Γ (mm/s)	χ^2	Mean bond length (Å)	Mean coordination number
Sb_2S_3	100.0	− 6.19(1)	10.7(2)	1.43(4)	1.45	2.64	4.0
$TlSb_5S_8$	83.3	− 5.25(2)	12.0(2)	1.551(9)	1.31	2.56	3.5
$TlSb_3S_5$	75.0	− 4.73(2)	12.5(4)	1.70(7)	1.33	2.54	3.3
$TlSbS_2$	50.0	− 4.42(2)	12.7(3)	1.61(7)	1.42	2.55	3.5
Tl_3SbS_3	25.0	− 3.30(2)	11.1(4)	1.19(7)	0.90	2.43	3.0

Note. Uncertainties in the last digit of the parameters are given in parentheses.

characteristic for Sb(III) species (12). All compounds have positive values of eQV_{zz}. Since the term eQ is negative for the isotope ^{121}Sb, the sign of the principal component of the electric field gradient V_{zz} is negative in all cases. This fact indicates an imbalance in the antimony 5*p* orbital occupation with an excess of *p* electron density in the direction of the principal component of the electric field gradient. In the following, we will focus our discussion almost exclusively on the changes of the isomer shift.

In the first section we will present and discuss the results obtained for several crystalline compounds of the system Sb_2S_3–Tl_2S, for which precise crystallographic data are available. In the second section, we will use these results for the interpretation of the data obtained for vitreous samples.

4.1. Crystalline Compounds of the Sb_2S_3–Tl_2S Binary System

The isomer shift δ of crystalline compounds of the Sb_2S_3–Tl_2S binary system decreases with increasing Sb_2S_3 concentration as shown in Table 1. Several attempts have been made to correlate variations of the isomer shift with modifications of the antimony environment. Lefebvre *et al.* (28, 29) have studied five specific compounds (SbI_3, Sb_2Te_3, SbTeI, $TlSbS_2$, and Tl_3SbS_3) by tight-binding band-structure calculations and molecular models combined with X-ray diffraction and photoemission spectroscopy to explain the observed trends in the ^{121}Sb Mössbauer isomer shift. They concluded that the isomer shift could be related to the number of missing ligands in octahedra around the

TABLE 2

Composition of the Amorphous Samples

Vitreous compounds	% Sb_2S_3	% As_2S_3	% Tl_2S	δ (mm/s)	eQV_{zz} (mm/s)	Γ (mm/s)	χ^2
1A	80	20	0	− 4.86(2)	11.7(3)	1.86(6)	1.68
2A	75	25	0	− 4.809(9)	11.8(1)	1.61(3)	2.39
3A	60	40	0	− 4.80(2)	12.1(1)	1.58(6)	1.24
4A	50	50	0	− 4.76(2)	12.1(2)	1.61(4)	1.47
5A	40	60	0	− 4.73(1)	12.5(3)	1.57(7)	1.13
6A	25	75	0	− 4.689(9)	12.8(1)	1.54(3)	2.52
13A	80	0	20	− 4.73(3)	14.5(5)	2.41(11)	1.37
20A	70	10	20	− 4.72(1)	12.7(2)	1.56(5)	2.04
21A	50	30	20	− 4.86(2)	12.9(3)	1.68(7)	1.72
22A	30	50	20	− 4.91(2)	11.9(4)	1.70(8)	1.33
23A	20	60	20	− 5.00(3)	12.8(5)	1.60(10)	1.22
24A	10	70	20	− 5.12(3)	11.1(4)	1.43(9)	1.27
25A	5	75	20	− 5.16(2)	9.5(4)	1.32(9)	1.20
30A	40	20	40	− 4.58(2)	12.6(3)	1.55(6)	1.82
31A	20	40	40	− 4.89(3)	11.2(5)	1.62(11)	1.38
32A	10	50	40	− 5.06(3)	10.0(6)	1.53(12)	1.32

Note. Summary of isomer shifts, δ (with respect to InSb), electric quadrupole coupling constants, eQV_{zz}, and linewidth, Γ, resulting from a least-squares analysis of the Mössbauer data for the vitreous compounds of the Sb_2S_3–As_2S_3–Tl_2S ternary system. Uncertainties in the last digit(s) of the parameters are given in parentheses.

antimony atom, and they explained the $5s^2$ nonbonding electron activity by an electronic loss that is always less than 0.1 electron. Bychkov and Wortmann (13) studied the local environment of antimony in several glasses using ^{121}Sb Mössbauer spectroscopy. They related the isomer shift to the mean Sb–S bond length. These two approaches seem incomplete to us.

For all five crystalline compounds, the mean bond length and the mean coordination number of antimony are indicated in Table 1. We do not observe a simple relation between the isomer shift and one of two other parameters (mean bond length and mean coordination number). We can conclude that the evolution of the isomer shift is not explained by the variations of the mean bond length or of the mean number coordination of antimony. Therefore, we defined an empirical bond length valence (EBLV) using the notion of bond valence with the following relation:

$$\text{EBLV} = \frac{\sum_{i=0}^{i} R_i (R_i/2.43)^{-5/2}}{\sum_{i=0}^{i} (R_i/2.43)^{-5/2}}. \qquad [3]$$

The EBVL represents the barycentric bond length for the various bond valences of antimony environments. The calculated EBLV for the five crystalline compounds varies almost linearly with the isomer shift, as shown in Fig. 3. Hence we can determine between the EBLV and the isomer shift the following relation:

$$\text{EBLV} = 2.18 - 0.082\delta \text{ (mm/s)}. \qquad [4]$$

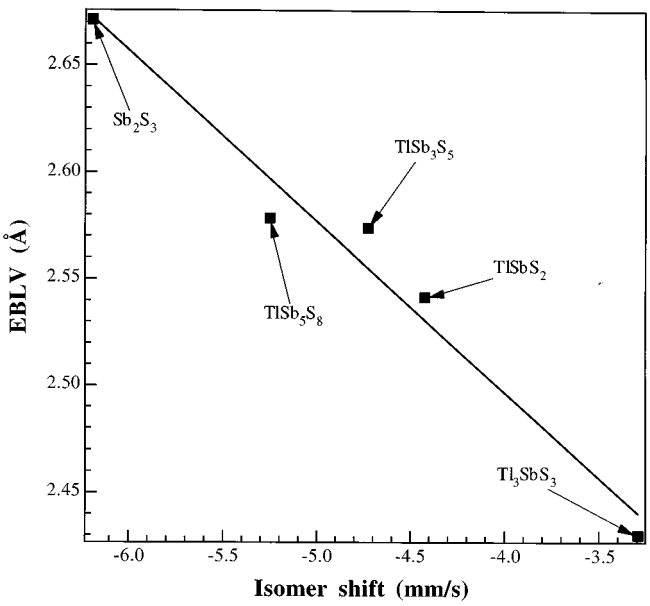

FIG. 3. Variation of the empirical bond length valence (EBLV) with the isomer shift for the crystalline compounds of the Sb_2S_3–Tl_2S binary system.

This linear relation demonstrates the importance of the weak bonds for the isomer shift. This parameter is therefore sensitive to both the strong and the weak bonds, but the influence of the strong bonds is more important. The influence of the weak bonds on the isomer shift complicates the interpretation of results. The increase of EBLV indicates a decrease of the covalent bond character, which, in turn, is related to a decrease of the stereochemical activity of the $5s^2$ nonbonding electrons. Two explanations of such an increase are possible:

(i) by increasing lengths of the strong bonds and decreasing lengths of the weak bonds in agreement with the interpretation of Bychkov and Wortmann (13) if we suppose that the antimony environment remains unchanged;

(ii) by an increase of the number of strong bonds in agreement with the interpretation of Lefebvre *et al.* (28, 29) if we suppose that the antimony environment is changed.

It seems difficult to distinguish the two cases without the use of other experimental methods. In the present study, XAFS is used as complementary technique.

4.2. *Vitreous Compounds*

(*a*) *The Sb_2S_3–As_2S_3 binary system.* The isomer shift δ for vitreous compounds of the Sb_2S_3–As_2S_3 binary system decreases linearly with increasing Sb_2S_3 concentration, from -4.69 mm/s (25% Sb_2S_3) to -4.86 mm/s (80% Sb_2S_3), as shown in Fig. 4. The extrapolation of the isomer shift to 100% Sb_2S_3 gives the value -4.90 mm/s. This is by 1.30 mm/s more positive than the isomer shift of the crystalline compound Sb_2S_3 and close to that of amorphous Sb_2S_3 (30).

The electric quadrupole coupling constant eQV_{zz} decreases also linearly with increasing Sb_2S_3 concentration from 12.8 mm/s (25% Sb_2S_3) to 11.7 mm/s (80% Sb_2S_3) as shown in Fig. 4. The extrapolation of this parameter to 100% Sb_2S_3 gives the value 11.3 mm/s. The composition dependency of these two Mössbauer parameters is in contradiction to the phase separation model for the Sb_2S_3–As_2S_3 binary system proposed previously by Kawamoto *et al.* (31). This model supposes that the Mössbauer parameters (isomer shift and electric quadrupole coupling constant) are independent to the composition and close to those of Sb_2S_3 vitreous.

The isomer shifts for these vitreous compounds correspond to values of the EBLV (calculated with the Eq. [4]) from 2.55 Å (25% Sb_2S_3) to 2.57 Å (80% Sb_2S_3). On one hand, the previous studies by XAFS at different edges (8–10) and by far-infrared transmission (11) have shown that the Sb_2S_3–As_2S_3 binary system is characterized by a random substitution of arsenic by antimony. The mean Sb–S bond length obtained by EXAFS at the antimony L_{III}-edge (9) for the vitreous compounds varied slightly from 2.50 Å (25% Sb_2S_3) to 2.51 Å (75% Sb_2S_3). If we consider, in agreement

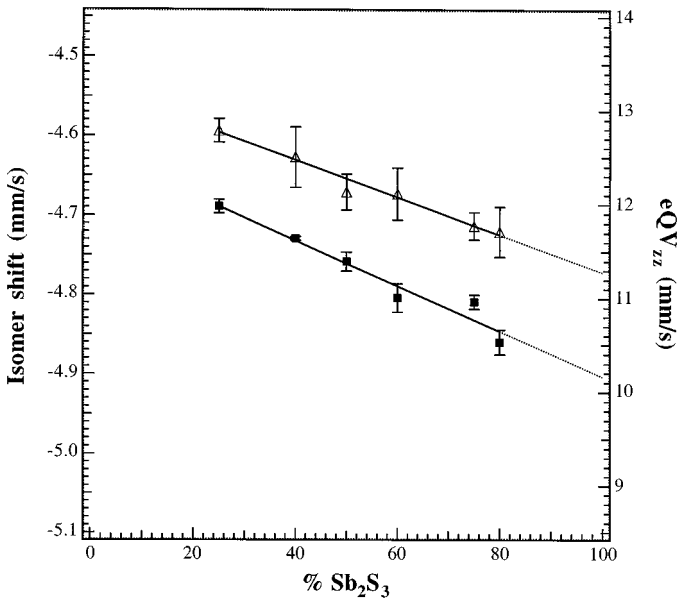

FIG. 4. Variation of the isomer shift (■) and of the electric quadrupole constant eQV_{zz} (△) with the Sb_2S_3 concentration for the vitreous compounds of the Sb_2S_3–As_2S_3 system.

with the previous studies, three bonds with lengths close to 2.51 Å, the values obtained for the sum of the EBV and for the EBLV are 2.4 (calculated with Eq. [2]) and 2.51 Å (calculated with Eq. [3]), respectively. To obtain values close to 3.0 (the sum of the EBV around each atom must be equal to the atom valence) and 2.56 Å, respectively, we must consider one or two weak bonds in antimony environments.

On the other hand, the linear variation of the EBLV on the Sb_2S_3–As_2S_3 vitreous system can easily be explained by the model of random substitution of arsenic by antimony. Indeed, the As–S bond lengths (2.29 Å (8)) in vitreous As_2S_3 are by 0.22 Å shorter than the Sb–S bond lengths (2.51 Å (9)) in vitreous Sb_2S_3. If we suppose a random substitution of arsenic by antimony, we can explain the contraction of Sb–S structural units together with a corresponding decrease of Sb–S strong bond lengths and an increase of Sb–S weak bond lengths by the more compact glass network at higher arsenic concentrations.

Cervinka and Hruby (32) by a comparison of radial density distribution curves for As_2X_3 (X = S, Se, Te) and Sb_2S_3 vitreous compounds have shown that the Sb_2S_3 vitreous compound belongs to the class of vitreous As_2X_3 structures and that in the series As_2S_3–As_2Se_3–As_2Te_3, a gradual transition from a layer-like to a random network takes place and that vitreous Sb_2S_3 can be put beside As_2S_3. Our previous studies gave indication that the As_2S_3 vitreous compound has a structure close to its crystalline compound. In crystalline As_2S_3 arsenic is found on two similar crystallographic sites with three short bonds (with lengths between 2.24 and 2.31 Å) and three long bonds (with lengths between 3.22 and 3.57 Å). These weak bonds provide the cohesion between the successive layers. Cervinka and Hruby (32) have constructed a simple model of vitreous Sb_2S_3. In this model the explanation of the non-zero electron density of the radial electron density distribution curve in the region of 3 Å, was achieved by a suitable mutual orientation of elementary SbS_3E units shown in Fig. 5. The Sb–S bond length (dotted line in Fig. 5b) is close to 3.1 Å. In agreement with the model of Cervinka and Hruby (32), our ^{121}Sb Mössbauer study reveals that antimony has three strong bonds and one or two weak bonds (with bond lengths between 2.90 and 3.20 Å). The sequences of pyramidal SbS_3E units with weak bonds lead to a gradual transition from the layer-like As_2S_3 structure to a random network for the Sb_2S_3–As_2S_3 binary system. Moreover, the linear increase of the glass transition temperature (8) from 481 K (100% As_2S_3) to 494 K (75% Sb_2S_3–25% As_2S_3) seems to confirm the gradual transition.

(*b*) *The Sb_2S_3–As_2S_3–Tl_2S ternary system.* Two series of samples were examined, one with a constant concentration of 20% Tl_2S and another with 40% Tl_2S. In contrast to the Sb_2S_3–As_2S_3 binary system, the isomer shift δ and the electric quadrupole coupling constant eQV_{zz} increase roughly with Sb_2S_3 concentration for both series of samples, as shown in Fig. 6 and Table 2. For the line of 20% Tl_2S concentration, the isomer shift does not vary linearly with Sb_2S_3 concentration. We can distinguish two ranges. In the first range, between 5% and 30% Sb_2S_3, the isomer shift depends strongly on the composition and varies from -5.16 mm/s (5% Sb_2S_3) to -4.91 mm/s (30% Sb_2S_3). In

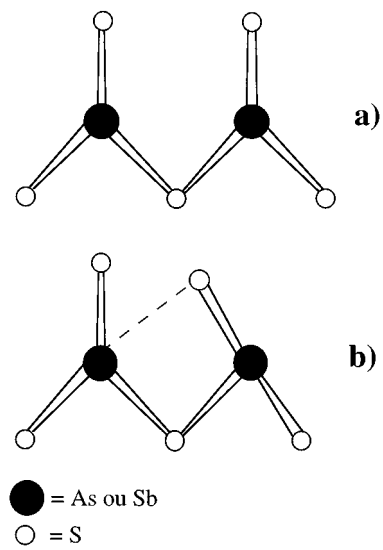

FIG. 5. Schematic figures of (a) two associated pyramidal AsS_3E units and of (b) basic mutual orientations of two associated pyramidal SbS_3E units.

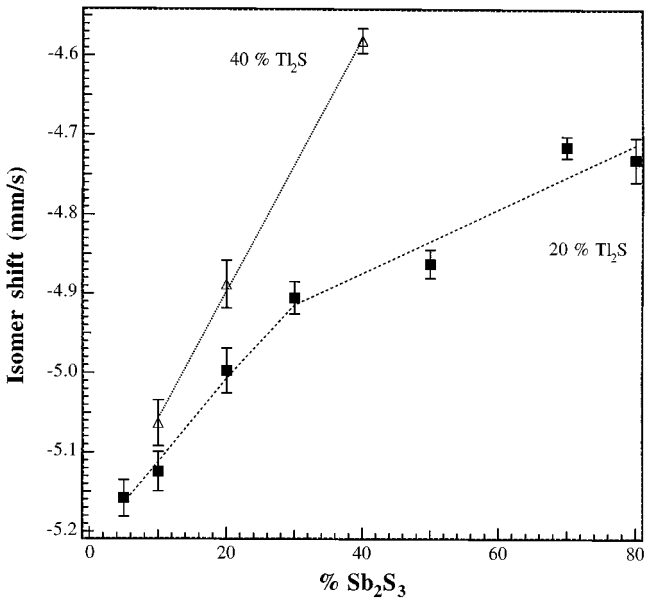

FIG. 6. Variation of the isomer shift with the Sb_2S_3 concentration in the Sb_2S_3–As_2S_3–Tl_2S ternary system at constant Tl_2S concentrations of 20% (■) and 40% (△).

the second range, above 30% Sb_2S_3 concentration, the isomer shift is somewhat less affected by the composition and varies from -4.91 mm/s (30% Sb_2S_3) to -4.73 mm/s (80% Sb_2S_3). The line of 40% Tl_2S concentration shows one range of strong variation of the isomer shift from -5.06 mm/s (10% Sb_2S_3) to -4.58 mm/s (40% Sb_2S_3).

The increase of the isomer shift with the Sb_2S_3 concentration for both series cannot be attributed to a decrease of the mean bond length alone. According to the previous XAFS studies (8–10) a decrease of the mean coordination number must be taken into account additionally. The two ranges of the isomer shift on the line of 20% Tl_2S are explained by the nonlinear variation of the mean coordination number with the Sb_2S_3 concentration. Indeed, in the vitreous compound 80% As_2S_3–20% Tl_2S in agreement with the previous EXAFS study at the arsenic K-edge, 15% of the sulfur bonds are S–As terminal bonds. The first range is therefore characterized by the elimination of the S–As terminal bonds in an already Tl_2S-doped As_2S_3 matrix by virtue of the formation of Sb–S–As bridges with SbS_4E and SbS_5E units. The second range can be characterized in the following way: the increase of the Sb_2S_3 content in a vitreous matrix consisting of numerous SbS_4E and SbS_5E units consists principally of the pyramidal-type SbS_3E involving a slight decrease of the mean coordination number. On the line of 40% Tl_2S concentration, the variation of the isomer shift is more important because in the starting vitreous compound (60% As_2S_3–40% Tl_2S) the sulfur atoms have more S–As terminal bonds (36% of the sulfur bonds) than the starting sample with the 20% Tl_2S line. The rough increase of the electric quadrupole constant eQV_{zz} with Sb_2S_3 concentration observed for both series may be attributed, according to the evolution of the isomer shift, to the increase of the activity of the $5s^2$ nonbonding electrons.

5. CONCLUSION

The interpretation of data from ^{121}Sb Mössbauer spectroscopy is difficult due to the various environment types found for the antimony atoms and due to the large distribution of bond lengths. Hence, to interpret the results, we determined the EBV for the pair (Sb, S) by using the work of Brown (19). For the determination of this value, we took all Sb–S bonds with lengths smaller than 3.2 Å into account. In addition, we defined an EBLV on the basis of the EBV. A linear relation between this notion and the isomer shift is found for the five crystalline compounds of the Sb_2S_3–Tl_2S binary system. The EBLV is a measure of the covalent bond character which can be related to the stereochemical activity of the $5s^2$ nonbonding electrons. This is a very interesting parameter because its use allowed us the interpretation of ^{121}Sb Mössbauer spectra. The isomer shift is found to be a very sensitive parameter of the strong bonds and of the weak bonds (with bond lengths between 2.90 and 3.20 Å).

In all vitreous compounds of the Sb_2S_3–As_2S_3–Tl_2S ternary system, antimony exists only as Sb(III) species with a stereochemical activity of the $5s^2$ nonbonding electrons. The variations of the isomer shift are attributed to structural changes in the environment of the antimony atoms, in particular to changes in the mean coordination number and the mean Sb–S bond length in agreement with previous XAFS studies (8–10).

In the Sb_2S_3–As_2S_3 system, the decrease of the isomer shift with increasing Sb_2S_3 concentration can be attributed to the increase of the mean Sb–S bond length in the SbS_3E pyramidal environments. In agreement with the study of Cervinka and Hruby (32), we demonstrated the existence of weak bonds around 3.0 Å in the antimony environments. This present study confirms that the sequence of pyramidal coordination patterns leads to the gradual transition from layer-like to a random network in this system.

In the Sb_2S_3–As_2S_3–Tl_2S ternary system on the two lines of constant concentrations of 20% and 40% Tl_2S, the increase of the isomer shift with the Sb_2S_3 concentration is assigned to the decrease of the mean coordination number. The presence of Tl_2S in the As_2S_3 matrix favors the formation of Sb–S–As bridges with SbS_4E and SbS_5E, reducing in this way the number of S–As terminal bonds. As the ratio between bridging and nonbridging bonds influences the properties of such glasses, the variation of the Sb_2S_3 and Tl_2S concentrations offers the possibility to synthesize glasses with predetermined properties.

ACKNOWLEDGMENTS

This research was carried out within the framework of the GDRE "Chalcogenures" of the CNRS. The authors thank M. L. Elidrissi Moubtassim and T. Barancira for their assistance with the Mössbauer measurements. We are grateful to M. Womes for the numerous discussions during the drafting of this manuscript. One of the authors (J.M.D.) thanks Professor G. Langouche for the hospitality during the stay at the Instituut voor Kern- en Stralingsfysika and gratefully acknowledges the Katholieke Universiteit Leuven for providing financial support.

REFERENCES

1. J. S. Sanghera, J. Heo, and J. D. MacKenzie, *J. Non-Cryst. Solids* **103,** 155 (1988).
2. T. Katsuyama and H. Matsumura, *J. Non-Cryst. Solids* **139,** 177 (1992).
3. S. R. Jagtap and J. K. Zope, *J. Non-Cryst. Solids* **127,** 19 (1991).
4. D. Gomez-Vela, L. Esquivias, and C. Prieto, *J. Non-Cryst. Solids* **167,** 59 (1994).
5. E. Sagbo, D. Houphouet-Boigny, R. Eholie, J.-C. Jumas, J. Olivier-Fourcade, M. Maurin, and J. Rivet, *J. Solid State Chem.* **113,** 145 (1994).
6. O. Savadogo, and K. C. Mandal, *Appl. Phys. Lett.* **63,** 228 (1993).
7. A. Bouaza, J. Olivier-Fourcade, J.-C. Jumas, M. Maurin, and H. Dexpert, *J. Chim. Phys.* **86,** 1579 (1989).
8. J.-M. Durand, J. Olivier-Fourcade, J.-C. Jumas, M. Womes, and P. Parent, *J. Mat. Sci.* **32** (1997). [in press]
9. J.-M. Durand, P. E. Lippens, J. Olivier-Fourcade, J.-C. Jumas, and M. Womes, *J. Non-Cryst. Solids* **194,** 109 (1996).
10. J.-M. Durand, P. E. Lippens, J. Olivier-Fourcade, J.-C. Jumas, and M. Womes, *J. Non-Cryst. Solids* **208,** 36 (1996).
11. M. A. El Idrissi-Raghni, J.-M. Durand, B. Bonnet, L. Hafid, J. Olivier-Fourcade, and J.-C. Jumas, *J. Alloys Comp.* **239,** 8 (1996).
12. J. Olivier-Fourcade, A. Ibanez, J.-C. Jumas, M. Maurin, I. Lefebvre, P. Lippens, M. Lannoo, and G. Allan, *J. Solid State Chem.* **87,** 366 (1990).
13. E. Bychkov and G. Wortmann, *J. Non-Cryst. Solids* **159,** 162 (1993).
14. J. Heo, J. S. Sanghera, and J. MacKenzie, *J. Non-Cryst. Solids* **101,** 23 (1988).
15. L. Pauling, *in* "The Nature of the Chemical Bond," 3rd ed., p. 548. University of Cornell Press, Ithaca, NY, 1960.
16. W. H. Zachariesen, *Z. Kristallogr.* **80,** 137 (1931).
17. G. Donnay and R. Allman, *Am. Mineral.* **55,** 1003 (1970).
18. I. D. Brown and R. D. Shannon, *Acta Crystallogr. A* **29,** 266 (1973).
19. I. D. Brown, *J. Solid State Chem.* **11,** 214 (1974).
20. P. Bayliss and W. Nowacki, *Z. Kristallogr.* **135,** 308 (1972).
21. P. Engel, *Z. Kristallogr.* **151,** 203 (1980).
22. N. Rey, Ph.D. Thesis, Université Montpellier, France, 1984.
23. M. Gostojic, W. Nowacki, and P. Engel, *Z. Kristallogr.* **159,** 217 (1982).
24. N. Rey, J.-C. Jumas, J. Olivier-Fourcade, and E. Philippot, *Acta Crystallogr. C* **39,** 971 (1983).
25. N. Rey, J.-C. Jumas, J. Olivier-Fourcade, and E. Philippot, *Acta Crystallogr. Sect. C* **40,** 1655 (1984).
26. S. L. Ruby and G. K. Shenoy, *in* "Mössbauer Isomer Shift" (G. K. Shenoy and F. E. Wagner, Eds.), p. 617. North-Holland, Amsterdam, 1978.
27. M. Yanaga, K. Endo, H. Nakahara, S. Ikuta, T. Miura, M. Takahashi, and M. Takeda, *Hyperfine Inter.* **62,** 359 (1990).
28. I. Lefebvre, M. Lannoo, G. Allan, A. Ibanez, J. Olivier-Fourcade, J.-C. Jumas, and E. Beaurepaire, *Phys. Rev. Lett.* **59,** 2471 (1987).
29. I. Lefebvre, M. Lannoo, G. Allan, and L. Martinage, *Phys. Rev. B* **38,** 8593 (1988).
30. J. M. D. Coey, *J. Phys. C* **6,** 89 (1974).
31. Y. Kawamoto and S. Tsuchihashi, *Yogyo-Kyokai Shi* **7,** 328 (1969).
32. L. Cervinka and A. Hruby, *J. Non-Cryst. Solids* **48,** 231 (1982).